

## Beta-Delayed Proton Decay of $^{73}\text{Sr}$

J.C. Batchelder, D.M. Moltz, T.J. Ognibene, M.W. Rowe  
R.J. Tighe and J. Cerny

*Nuclear Science Division, Lawrence Berkeley Laboratory  
University of California, Berkeley, California 94720, USA*

October 1993

This work was supported by the Director, Office of Energy Research Division  
of Nuclear Physics of the Office of High Energy and Nuclear Physics of the  
U.S. Department of Energy under Contract DE-AC03-76SF00098



## Beta-Delayed Proton Decay of $^{73}\text{Sr}$

J. C. Batchelder, D. M. Moltz, T. J. Ognibene, M. W. Rowe, R. J. Tighe and  
Joseph Cerny

Department of Chemistry and  
Lawrence Berkeley Laboratory  
University of California  
Berkeley, California 94720

The  $T_z = -3/2$ ,  $A = 4n + 1$  nuclide  $^{73}\text{Sr}$  produced in the  $^{40}\text{Ca} (^{36}\text{Ar}, 3n)$  reaction has been observed via beta-delayed proton emission. A single proton group at a laboratory energy of  $3.75 \pm 0.04$  MeV has been observed, corresponding to decay of the  $T = 3/2$  isobaric analog state in  $^{73}\text{Rb}$  to the ground state of  $^{72}\text{Kr}$ . Combining this measurement with a Coulomb displacement energy calculation yields a mass excess for  $^{73}\text{Sr}$  of  $-31.82 \pm 0.24$  MeV based on a predicted mass for  $^{72}\text{Kr}$  of  $-53.94 \pm 0.24$  MeV.

## Introduction

Experiments involving the observation of neutron-deficient nuclei near the proton drip line have often proven difficult due to the small production cross-sections and high beta backgrounds. However, the unique signature of beta-delayed proton emission allows these nuclei to be detected in a very high beta background arising from nuclides that lie closer to the valley of stability. The use of  $Z = N$  targets and beams permits one to produce the heavier members of the  $A = 4n + 1$ ,  $T_z = -3/2$  series through the three neutron exit channel. Figure 1 shows a section of the chart of the nuclides in the  $Z = 31$  to 41 region, showing the lightest nuclide of each element that has been observed using projectile fragmentation methods<sup>1,2</sup>, and those nuclei which have been discovered via their beta-delayed proton branch: the  $A = 4n + 1$ ,  $T_z = +1/2$  series  $^{65}\text{Ge}$ <sup>3,4,5</sup>,  $^{69}\text{Se}$ <sup>4,6</sup>,  $^{73}\text{Kr}$ <sup>3,4</sup>,  $^{77}\text{Sr}$ <sup>6</sup>,  $^{81}\text{Zr}$ <sup>7</sup> and the  $A = 4n + 1$ ,  $T_z = -3/2$  series  $^{61}\text{Ge}$ <sup>8</sup>,  $^{65}\text{Se}$ <sup>9</sup>, and (as reported in this paper)  $^{73}\text{Sr}$ . All of the nuclei in the  $A = 4n+1$ ,  $T_z = -3/2$  series from  $^9\text{C}$  to  $^{65}\text{Se}$  are particularly favored by strong beta-delayed proton branches ranging from 11 to 100%<sup>8,9,10</sup>.

Above  $^{65}\text{Se}$ , the next higher member of this series,  $^{69}\text{Kr}$ , is also predicted to undergo beta-delayed proton emission, but Kr is a noble gas and therefore cannot be efficiently transported and collected via the helium-jet technique used in this work. It could be observed utilizing a detection system such as that used to observe  $^{33}\text{Ar}$ <sup>11</sup>. Thus,  $^{73}\text{Sr}$ , the next member in the series, becomes the obvious choice for study.  $^{73}\text{Sr}$  has been predicted by all the mass formulas

in the 1988 mass tables<sup>12</sup> to be bound to ground state proton emission. The lightest Sr isotope previously known to be particle stable is  $^{75}\text{Sr}$  <sup>1</sup>, and the lightest Sr isotope whose beta decay has been studied is  $^{77}\text{Sr}$  <sup>4,13</sup>. Proton-emitting transitions in the heavier nuclei are dominated by the decay to the isobaric analog state (IAS) in the beta daughter, readily permitting an estimation of the mass of the parent nucleus by using a formula for the Coulomb displacement energy to determine the difference in energy of the IAS and the parent ground state.

Due to the fact that  $^{40}\text{Ca}$  is the heaviest stable isotope with  $N = Z$ , this method for extending the  $T_z = -3/2$  series can only be used for one nucleus heavier than  $^{73}\text{Sr}$ , the next member of the series,  $^{77}\text{Zr}$ , which is also predicted to be a strong beta-delayed proton emitter. For production of even heavier members, the reaction would have to proceed through exit channels involving evaporation of five neutrons or more, with extremely small cross sections.

To predict the mass of a beta-delayed proton precursor, and its emitted proton energy from the daughter IAS, one can use the fact that the binding energies between mirror nuclei differ primarily by their respective Coulomb energies. Then the Kelson-Garvey mass relation<sup>14</sup> can be used to predict the masses of proton-rich nuclides with  $T_z \leq -1$ ; this method has proven to be the most effective in this region. The Kelson-Garvey mass relation requires as input the masses of the  $T_z = -1/2$  and  $T_z = +1/2$  nuclides. Although the masses of the  $T_z = -1/2$  members are not known, those of the corresponding neutron-rich mirrors are known (except for  $^{71}\text{Br}$ , for which we use the prediction<sup>12</sup> by Wapstra, Audi and Hoekstra, which utilizes

---

systematic mass trends). Then the masses of the  $T_z = -1/2$  nuclei have been predicted by utilizing a Coulomb displacement energy formula<sup>15</sup>. Using this method, the mass excess for  $^{73}\text{Sr}$  is calculated to be  $-31.54 \pm 0.62$  MeV. The large error is due to the errors in the measured masses associated with the known  $T_z = 1/2$  nuclei and those arising from the calculated  $T_z = -1/2$  nuclei. The above Coulomb displacement approach (with  $\Delta E_{\text{Coul}} = 11.03$  MeV) was also used to predict the mass of the IAS in the beta daughter  $^{73}\text{Rb}$ . (Previous searches for  $^{73}\text{Rb}$  have proven unsuccessful<sup>2,16</sup>, but its mass has been predicted by Wapstra *et al.*<sup>12</sup> to be  $-46.59 \pm 0.62$  MeV, which we adopt for future use.) Combining the predicted mass for  $^{72}\text{Kr}$  (from Wapstra *et al.*<sup>12</sup>) of  $-53.94 \pm 0.24$  MeV and that for the IAS in  $^{73}\text{Rb}$  yields a proton decay energy of  $4.03 \pm 0.67$  MeV (in the laboratory frame).

### Experimental method

$^{73}\text{Sr}$  was produced via the  $^{40}\text{Ca}(^{36}\text{Ar},3n)$  reaction using a 245 MeV  $^{36}\text{Ar}^{8+}$  beam from the Lawrence Berkeley Laboratory 88-Inch Cyclotron, which was degraded by the He-jet entrance window assembly to an on-target energy of 140 MeV. The He-jet transport system that was employed in this experiment is shown schematically in Fig. 2. Beam current, which was limited by the energy loss in the Havar windows, was typically 800 enA. Recoil nuclei from a  $1.9 \text{ mg/cm}^2$  natural Ca target were transported on KCl aerosols in the helium, through a 75 cm long capillary (1.4 mm i.d.) to a shielded detector chamber. The total transit time for this system was  $\sim 25$  ms. The recoils were deposited on a slowly

rotating wheel which was then viewed directly by two Si-Si detector telescopes situated above and below the wheel and  $120^\circ$  apart. Each telescope subtended a solid angle of 4% of  $4\pi$  at a distance of 5 mm from the wheel. The wheel speed was varied to minimize the long lived beta background. Calibration of these telescopes was accomplished by using beta-delayed protons from  $^{25}\text{Si}^{17}$  which were produced in the  $^{24}\text{Mg}(^3\text{He},2n)$  reaction at  $E_{^3\text{He}} = 40$  MeV.

## Results

There were two separate experiments detecting  $^{73}\text{Sr}$ , which utilized  $\Delta E$  detectors of differing thickness. The first experiment utilized telescopes each of which consisted of a  $75\ \mu\text{m}$   $\Delta E$  and a  $300\ \mu\text{m}$  E. These telescopes had a resolution of 100 keV. Figure 3 shows the delayed-proton energy spectrum from one of these telescopes (the top telescope was not working in this experiment) at a wheel speed of 27 seconds per revolution arising from the bombardment of 49 mC of 140 MeV  $^{36}\text{Ar}^{8+}$  on a  $^{\text{nat}}\text{Ca}$  target.

This spectrum clearly shows a peak containing 21 counts at  $3.77 \pm 0.05$  MeV, which, as discussed below, we assign to the beta-delayed proton decay of  $^{73}\text{Sr}$ . The spectrum also contains 8 events at 4.7 MeV due to the "100%"  $^{41}\text{Ti}^{18}$  transition (arising from transfer reactions on the Ca target), as well as events up to  $\sim 3.1$  MeV due to  $^{69}\text{Se}^{4,6}$ , and  $^{77}\text{Sr}^6$  (due to reactions on  $^{42,44}\text{Ca}$ ).  $^{41}\text{Ti}$  also has transitions at 3.69 MeV (15.5%), and at 3.75 MeV (31.0%). (These percentages are relative to the intensity of the strongest observed proton transition). However, only  $4 \pm 2$  events due to  $^{41}\text{Ti}$

would be expected at  $\sim 3.75$  MeV. A few counts of  $^{65}\text{Se}$  are expected at  $3.55$  MeV<sup>9</sup>, although the background in this spectrum is too high to determine this.

The second experiment utilized telescopes each consisting of a  $27\ \mu\text{m}$   $\Delta E$  and a  $300\ \mu\text{m}$  E, with resolutions of  $\sim 45$  keV. A summed spectrum from both telescopes which was taken at the same wheel speed as before and which arose from a bombardment of  $35$  mC is shown in Fig. 4a. This spectrum again shows a peak at  $3.73 \pm 0.05$  MeV containing 11 events. The composite spectrum reveals a contribution due to  $^{37}\text{Ca}$ <sup>18</sup> (formed via transfer reactions on the Ca target), a small peak at  $3.5$  MeV arising from  $^{65}\text{Se}$ <sup>9</sup>, a small peak at  $4.7$  MeV due to  $^{41}\text{Ti}$ <sup>18</sup> (again formed via transfer reactions) as well as lower energy protons arising from the decays of  $^{69}\text{Se}$  and  $^{77}\text{Sr}$ . The events near  $3.85$  MeV are hard to attribute to any likely transition. The 100%  $^{41}\text{Ti}$  peak contains 5 events implying that  $2 \pm 2$  events from  $^{41}\text{Ti}$  would be expected in the region of  $3.75$  MeV. For comparison, a generated spectrum for  $^{41}\text{Ti}$  using the experimental resolution and known peak ratios<sup>18</sup> is shown in Fig. 4b. Figure 4c indicates the contribution from  $^{41}\text{Ti}$  to the total spectrum (from 4a), which clearly shows that the peak at  $3.73$  MeV could not have arisen from the decay of this nucleus. We therefore assign this peak to the beta-delayed proton emission of  $^{73}\text{Sr}$ . Combining the results from the two experiments gives an emitted proton energy of  $3.75 \pm 0.04$  MeV (in the laboratory frame) from the IAS of  $^{72}\text{Kr}$ .

To prove that this proton peak could not have arisen from  $^{69}\text{Kr}$ , or another lighter nuclide formed from a competing reaction channel, a  $^{\text{nat}}\text{Ca}$  target was bombarded with  $13$  mC of a  $195$  MeV  $^{32}\text{S}^{6+}$  beam



(degraded to 135 MeV at the target midpoint). This experiment was performed at the same wheel speed of 27 seconds per revolution, and utilized the same detector combinations of a 27  $\mu\text{m}$   $\Delta E$  and a 300  $\mu\text{m}$  E. The resulting delayed-proton spectrum, presented in Fig. 5a, shows that the only peaks seen at energies higher than 3 MeV are due to  $^{41}\text{Ti}$  and  $^{65}\text{Se}$ . For clarity, Fig. 5b shows the spectrum with the  $^{41}\text{Ti}$  events normalized to the 4.7 MeV peak subtracted. As noted above,  $^{69}\text{Kr}$  should not be efficiently transported by the He-jet.  $^{41}\text{Ti}$  is formed in the  $^{32}\text{S}(^{16}\text{O},\alpha 3n)$  reaction from oxygen contaminants in the target.

Although several channels in this experiment are open via either fusion evaporation or transfer reactions which could result in the production of other beta-delayed proton emitters (both from the Ca target and its contaminants (chiefly Mg and O)), the only other protons expected to appear above 3.5 MeV are from  $^{41}\text{Ti}$  and  $^{65}\text{Se}$ . Table 1 summarizes all known, non noble gas, beta-delayed proton emitters likely to be formed with emitted proton energies above 3.0 MeV. This shows that our measurement can exploit an energy window where no interference with the observation of delayed protons with energy greater than 3.5 MeV is expected except for  $^{41}\text{Ti}$  which is formed by transfer reactions on the target. (The decay of  $^{57}\text{Zn}$  <sup>19</sup> is not observed in the experimental spectra implying that the Mg contamination must be very small.)

The predicted cross-section using the statistical evaporation code ALICE <sup>20</sup> for  $^{73}\text{Sr}$  produced by a  $^{36}\text{Ar}$  beam of 140 MeV on a  $^{40}\text{Ca}$  target is 210 nb. However, ALICE has consistently over predicted the cross sections found in this region by as much as a

factor of 10 - 20<sup>9,21</sup>. The absolute efficiency for the He-jet system has been measured for  $^{61}\text{Ge}$  (which has a half life of 40 ms) to be ~5% with a single capillary, and this efficiency was assumed to be the same for Sr. Takahashi's gross theory of beta decay<sup>22</sup> predicts the half-life of  $^{73}\text{Sr}$  to be ~15 ms. Using this predicted half-life of 15 msec, the experimental cross-section for the  $^{40}\text{Ca}(^{36}\text{Ar},3n)^{73}\text{Sr}$  reaction is on the order of 20 nb. The ratio of the ALICE prediction to the observed value is ~10. This is consistent with the ratio found for the previously discovered members of the  $A = 4n + 1, T_z = -3/2$  series:  $^{61}\text{Ge}$ <sup>21</sup> (ratio = 11) and  $^{65}\text{Se}$ <sup>9</sup> (ratio = 18).

## Conclusions

A proposed partial decay scheme for  $^{73}\text{Sr}$  is shown in Fig. 6. The beta branching ratio to the IAS has been estimated assuming the superallowed transition has a  $\log ft = 3.3$ . The laboratory energy of the observed delayed proton peak from  $^{73}\text{Sr}$  is  $3.75 \pm 0.04$  MeV. Combining this result with the Coulomb displacement formula<sup>15</sup> and the Wapstra, Audi and Hoekstra predicted mass<sup>12</sup> of  $^{72}\text{Kr}$  ( $-53.94 \pm 0.24$  MeV) yields a mass excess for  $^{73}\text{Sr}$  of  $-31.82 \pm 0.24$  MeV. Although this predicted mass differs by 560 keV from that predicted by our use of the Kelson-Garvey mass relation, the two predictions agree within their associated large error bars.

Table 2 shows a comparison of the beta-delayed proton energy with predictions of selected theoretical models given in the 1988 mass tables<sup>12</sup>. Agreement within ~100 keV for the energy of the emitted proton is seen for the methods that use the Garvey-Kelson

and Kelson-Garvey mass relations as a basis for their predictions, namely the Comay-Kelson-Zidon and Jänecke-Masson predictions. Of the other mass formulas in Ref.12, the Masson-Jänecke prediction (inhomogeneous partial difference equation with higher order isospin contributions) also agrees excellently with the emitted proton energy reported in this work. The other three mass formulas, Tachibana *et al.* (empirical mass formula with a realistic proton-neutron interaction), Möller *et al.* (finite-range droplet model) and Möller-Nix (unified macroscopic-microscopic model) predict proton energies that are lower than the experimental value by ~800 to 1300 keV. These comparisons are consistent with the analysis reported earlier for  $^{65}\text{Se}$  <sup>9</sup>.

Table 3 presents a comparison of the known experimental data and the predictions of these mass theories for nuclei from  $^{61}\text{Ge}$  to  $^{77}\text{Zr}$  in the  $A = 4n+1$ ,  $T_z = -3/2$  series. The selected mass models all agree with each other fairly well for  $^{61}\text{Ge}$  (but are uniformly slightly lower than the experimental result). However, beginning with the next nucleus,  $^{65}\text{Se}$ , the values for the predictions diverge and cover a larger range, with this trend continuing up through  $^{77}\text{Zr}$ . For all four of these nuclides, the two methods based on the Kelson-Garvey mass relation (Comay-Kelson-Zidon and Jänecke-Masson) and the Masson-Jänecke predictions agree fairly well with one another, and also agree with the experimental data for  $^{65}\text{Se}$  and  $^{73}\text{Sr}$ . The other three methods, as noted above, under predict the emitted proton energy for  $^{65}\text{Se}$  and  $^{73}\text{Sr}$  (and predict energy values significantly less than those predicted by the Comay-Kelson-Zidon, Jänecke-Masson and the Masson-Jänecke mass predictions for the

unobserved nuclides  $^{69}\text{Kr}$  and  $^{77}\text{Zr}$ ). These results are a further justification for the use of a mass model based on systematic mass relations for nuclei far from stability in this region.

This work was supported by the Director, Office of Energy Research, Division of Nuclear Physics of the Office of High Energy and Nuclear Physics of the U.S. Department of Energy under Contract DE-AC03-76SF00098.

## REFERENCES

1. M. F. Mohar, D. Bazin, W. Benenson, D. J. Morrissey, N. A. Orr, B. M. Sherrill, D. Swan, J. A. Winger, A. C. Mueller, and D. Guillemaud-Mueller, *Phys. Rev. Lett.* **66**, 1571 (1991).
2. S. J. Yennello, J. A. Winger, T. Antaya, W. Benenson, M. F. Mohar, D. J. Morrissey, N. A. Orr, and B. M. Sherrill, *Phys. Rev. C* **46**, 2620 (1992).
3. J. C. Hardy, T. Faestermann, H. Schmeing, J. A. McDonald, H. R. Andrews, J.S. Geiger, and R. L. Graham, *Nucl. Phys.* **A371**, 349 (1981).
4. J. C. Hardy, J. A. McDonald, H. Schmeing, T. Faestermann, H. R. Andrews, J.S. Geiger, R. L. Graham, and K. P. Jackson, *Phys. Lett.* **B63**, 27 (1976).
5. K. Vierinen, *Nucl. Phys.* **A463**, 650 (1987).
6. J. A. McDonald, J. C. Hardy, H. Schmeing, T. Faestermann, H. R. Andrews, J.S. Geiger, R. L. Graham, and K. P. Jackson, *Nucl. Phys.* **A288**, 1 (1977).

7. J. C. Hardy, Proceedings of the 4th International Conference on Nuclei Far from Stability, Helsingør, Denmark, edited by P. G. Hansen and O. B. Nielson (CERN Report No. 81-09, CERN, Geneva, 1981) p. 217.
  8. M. A. C. Hotchkis, J. E. Reiff, D. J. Vieira, F. Blönnigen, T. F. Lang, D. M. Moltz, X. Xu, and J. Cerny, Phys. Rev. C **35**, 315 (1987).
  9. J. C. Batchelder, D. M. Moltz, T. J. Ognibene, M. W. Rowe, and J. Cerny, Phys. Rev. C **47**, 2038 (1993).
  10. J. Cerny and J. C. Hardy, Ann. Rev. Nucl. Sci. **27**, 333 (1977).
  11. J.C. Hardy, J.E. Esterl, R.G. Sextro, and J. Cerny, Phys. Rev. C **3**, 700 (1971).
  12. P. E. Haustein, At. Data Nucl. Data Tables **39**, 186 (1988).
  13. C. J. Lister, B. J. Varley, D. E. Alburger, P. E. Haustein, S. K. Saha, J. W. Olness, H. G. Price, and A. D. Irving, Phys. Rev. C **28**, 2127 (1983).
  14. I. Kelson and G. T. Garvey, Phys. Lett. **23**, 689 (1966).
  15. M. S. Antony, J. Britz, and A. Pape, At. Data Nucl. Data Tables **34**, 279 (1986).
  16. J. M. D'Auria, L. C. Carraz, P. G. Hansen, B. Jonson, S. Mattson, H. L. Ravn, M. Skoestad, and L. Westgaard, Phys. Lett. **B66**, 233 (1977).
  17. J. D. Robertson, D. M. Moltz, T. F. Lang, J. E. Reiff, J. Cerny, and B. H. Wildenthal, Phys. Rev. C **47**, 1455 (1993).
  18. R. G. Sextro, R. A. Gough, and J. Cerny, Nucl. Phys. **A234**, 130 (1974).
-

19. D. J. Vieira, D. F. Sherman, M. S. Zisman, R. A. Gough, and J. Cerny, Phys. Lett. **B60**, 261 (1976).
20. M. Blann and J. Birplinghoff, Lawrence Livermore National Laboratory report UCID-19614, unpublished (1982).
21. D. J. Vieira, Ph. D. thesis Lawrence Berkeley Laboratory report LBL-7161, 27 (1978), unpublished.
22. K. Takahashi, M. Yamada and T. Kondoh, At. Data Nucl. Data Tables **12**, 101 (1973).

Table 1. Non noble gas beta-delayed proton emitters formed in competing reactions with proton energies greater than 3.0 MeV (see text).

Nuclide	Reaction type	Emitted Proton Energy*
$^{37}\text{Ca}$	Transfer	$3.103 \pm 0.003$ MeV (100%)
		$3.173 \pm 0.010$ MeV (12.8%)
$^{41}\text{Ti}$	Transfer	$3.077 \pm 0.015$ MeV (60.3%)
		$3.690 \pm 0.015$ MeV (15.5%)
		$3.749 \pm 0.010$ MeV (31.0%)
		$4.187 \pm 0.015$ MeV (15.4 %)
		$4.734 \pm 0.004$ MeV (100%)
$^{57}\text{Zn}$	Fusion-evaporation from Mg contaminants	$1.92 \pm 0.05$ MeV (100%)
		$2.53 \pm 0.05$ MeV (50%)
		$4.57 \pm 0.05$ MeV (60%)
$^{61}\text{Ge}$	Fusion-evaporation	$3.10 \pm 0.03$ MeV (100%)
$^{65}\text{Se}$	Fusion-evaporation	$3.55 \pm 0.03$ MeV (100%)
$^{69}\text{Se}$	Fusion-evaporation	weak emitter with high energy tail up to 3.2 MeV
$^{77}\text{Sr}$	Fusion-evaporation	weak emitter with high energy tail up to 3.5 MeV

\* Percentages are relative to the intensity of the strongest observed proton transition.

Table 2. Comparison of the observed laboratory proton decay energy from the isobaric analog state vs. that predicted by selected mass models for  $^{73}\text{Sr}$  (all energies are given in MeV in the laboratory frame). All mass model predictions have been taken from Ref. 12.

	$\Delta(^{73}\text{Sr})$	$\Delta(^{72}\text{Kr})$	$E_{p(\text{lab})}^*$
Möller-Nix	-32.34	-53.66	2.96
Möller et al.	-32.58	-53.81	2.87
Tachibana et al.	-33.03	-53.82	2.45
Comay-Kelson-Zidon	-31.76	-53.94	3.81
Jänecke-Masson	-31.95	-54.23	3.90
Masson-Jänecke	-32.06	-54.22	3.79
Experimental			$3.75 \pm 0.04$

\* A constant value for  $\Delta E_{\text{Coul}} = 11.03$  MeV has been used.



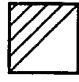




Table 3. Comparison of selected mass models for the beta-delayed proton energy\* from the IAS of the  $A = 4n + 1$ ,  $T_z = -3/2$  series nuclei:  $^{61}\text{Ge}$  through  $^{77}\text{Zr}$  (All energies are given in MeV in the laboratory frame). All mass model predictions have been taken from Ref. 12.

	$E_p(^{61}\text{Ge})$	$E_p(^{65}\text{Se})$	$E_p(^{69}\text{Kr})$	$E_p(^{73}\text{Sr})$	$E_p(^{77}\text{Zr})$
Möller-Nix	2.94	3.03	2.99	2.96	3.42
Möller et al.	2.94	2.98	2.97	2.87	3.32
Comay-Kelson-Zidon	2.89	3.50	3.74	3.81	4.04
Tachibana et al.	2.93	2.92	2.58	2.45	2.72
Jänecke-Masson	2.92	3.17	3.59	3.90	4.28
Masson-Jänecke	2.70	3.46	3.78	3.79	4.13
Experimental	$3.10 \pm 0.03$ a	$3.55 \pm 0.03$ b	$3.75 \pm 0.04$		

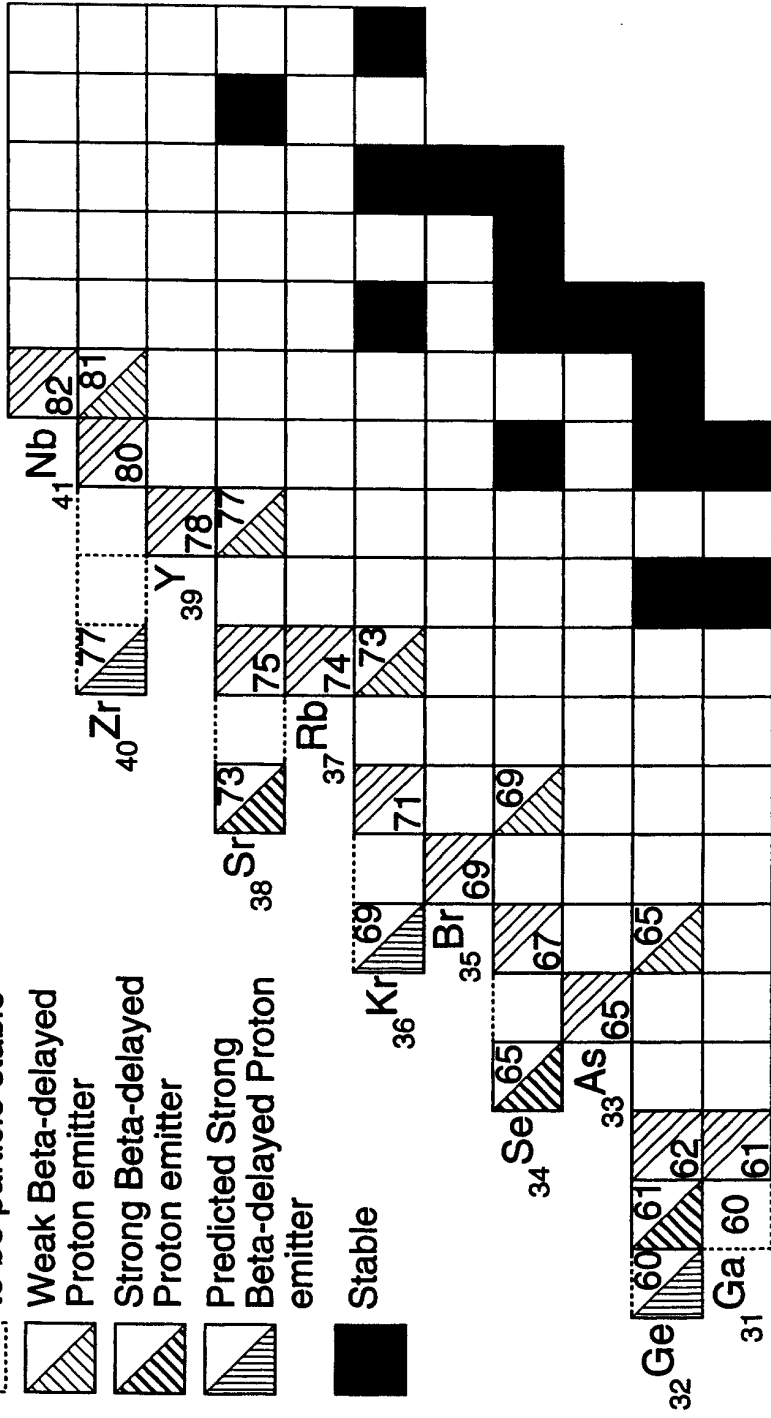
\* A constant value for  $\Delta E_{\text{Coul}}$  has been used for all predictions of each nucleus  
a. From Ref. 8.  
b. From Ref. 9.

Figure Captions

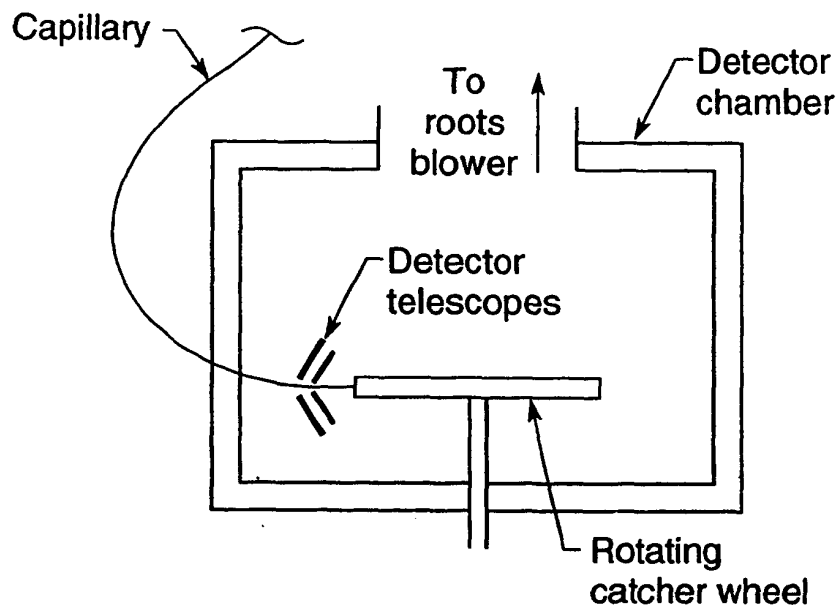
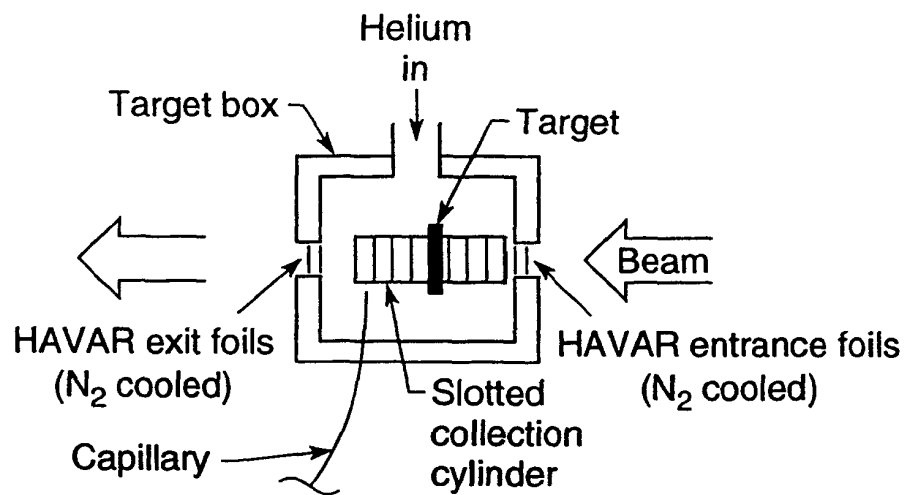
- Figure 1). Portion of the chart of the nuclides from  $Z = 31$  to  $Z = 41$  showing in part the lightest nuclide of a given element that has been identified by projectile fragmentation or by beta-delayed proton decay.
- Figure 2). Schematic diagram of the He-jet transport system and the basic telescope arrangement employed.
- Figure 3). Delayed proton spectrum resulting from the first experiment utilizing the 140 MeV  $^{36}\text{Ar} + \text{natCa}$  reaction with a  $75\ \mu\text{m}$   $\Delta E$ ,  $300\ \mu\text{m}$  E silicon detector telescope.
- Figure 4a). Delayed proton spectrum from the second experiment utilizing the 140 MeV  $^{36}\text{Ar} + \text{natCa}$  reaction and  $27\ \mu\text{m}$   $\Delta E$ ,  $300\ \mu\text{m}$  E silicon detector telescopes.
- 4b).  $^{41}\text{Ti}$  spectrum generated using the experimental resolution.
- 4c).  $^{41}\text{Ti}$  spectrum from b) normalized to the 4.7 MeV peak in a) and superimposed on spectrum a).
- Figure 5a) Delayed proton spectrum resulting from the 135 MeV  $^{32}\text{S} + \text{natCa}$  reaction.
- 5b) Delayed proton spectrum from Fig. 5a with events arising from the decay of  $^{41}\text{Ti}$  subtracted (see text).
- Figure 6) Proposed decay scheme for  $^{73}\text{Sr}$ . Energy levels are given relative to the ground state of  $^{72}\text{Kr}$ . The predicted masses of  $^{73}\text{Rb}$  ( $-46.59 \pm 0.62$  MeV) and  $^{72}\text{Kr}$  ( $-53.94 \pm 0.24$  MeV) are taken from the predictions of Wapstra *et al.* <sup>12</sup>.

-  Lightest isotope identified by projectile fragmentation
-  Lightest isotopes predicted to be particle stable
-  Weak Beta-delayed Proton emitter
-  Strong Beta-delayed Proton emitter
-  Predicted Strong Beta-delayed Proton emitter

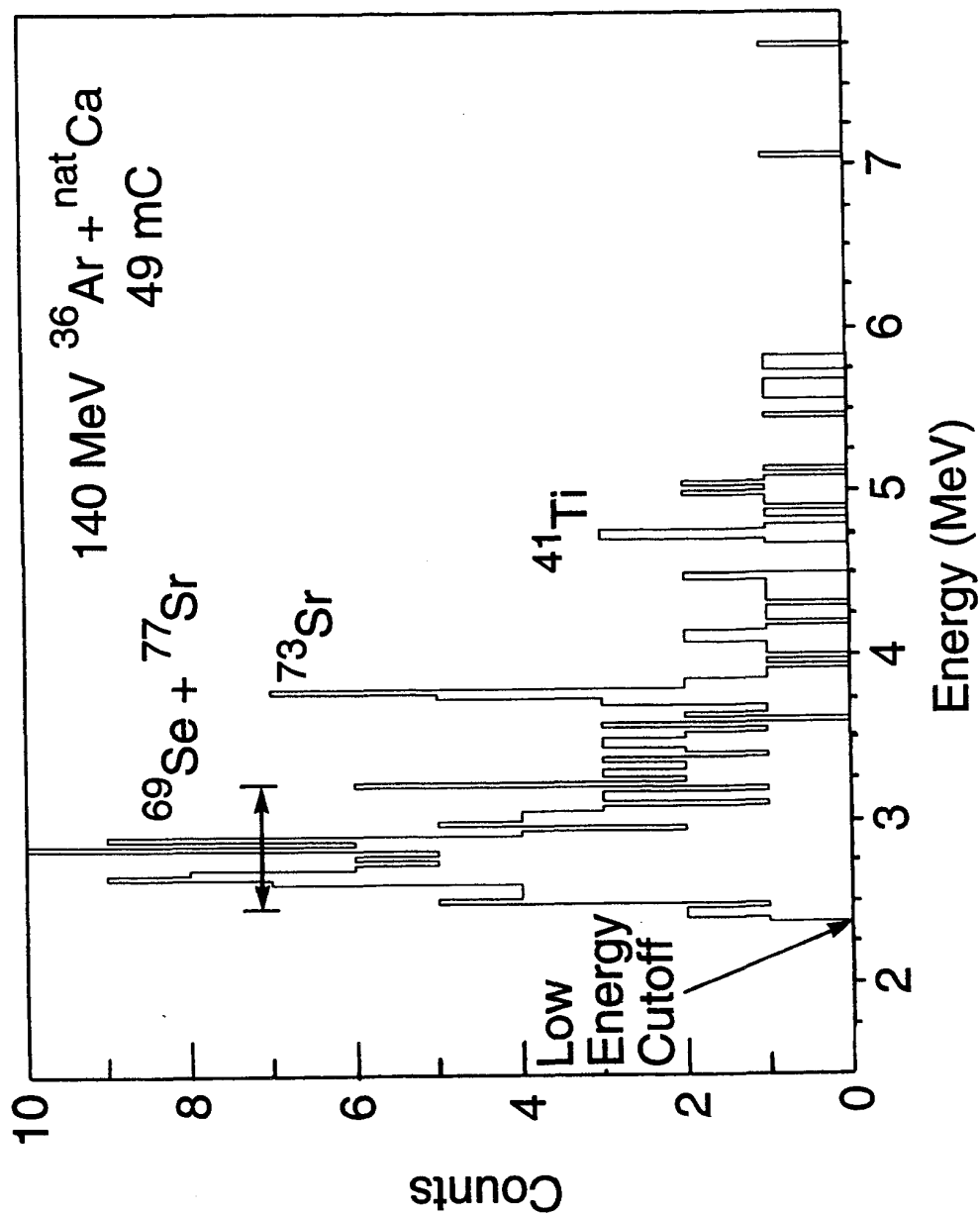
 Stable



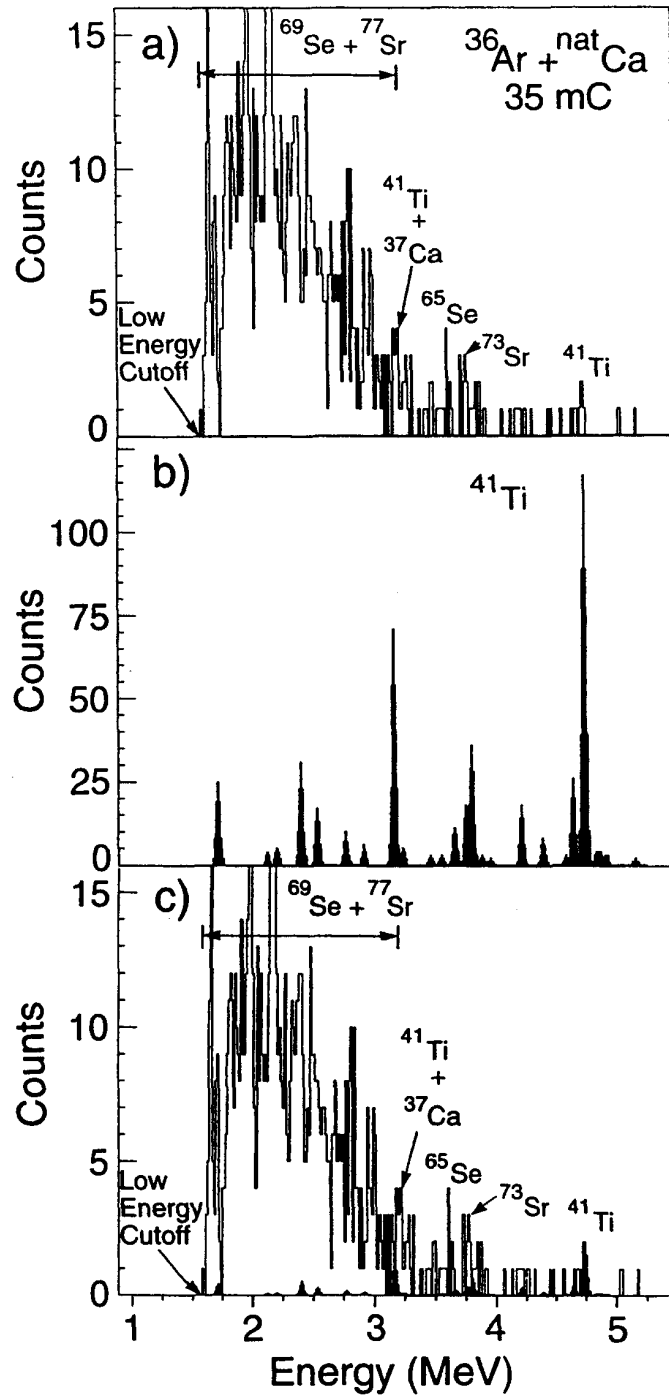
XBL 936-4054



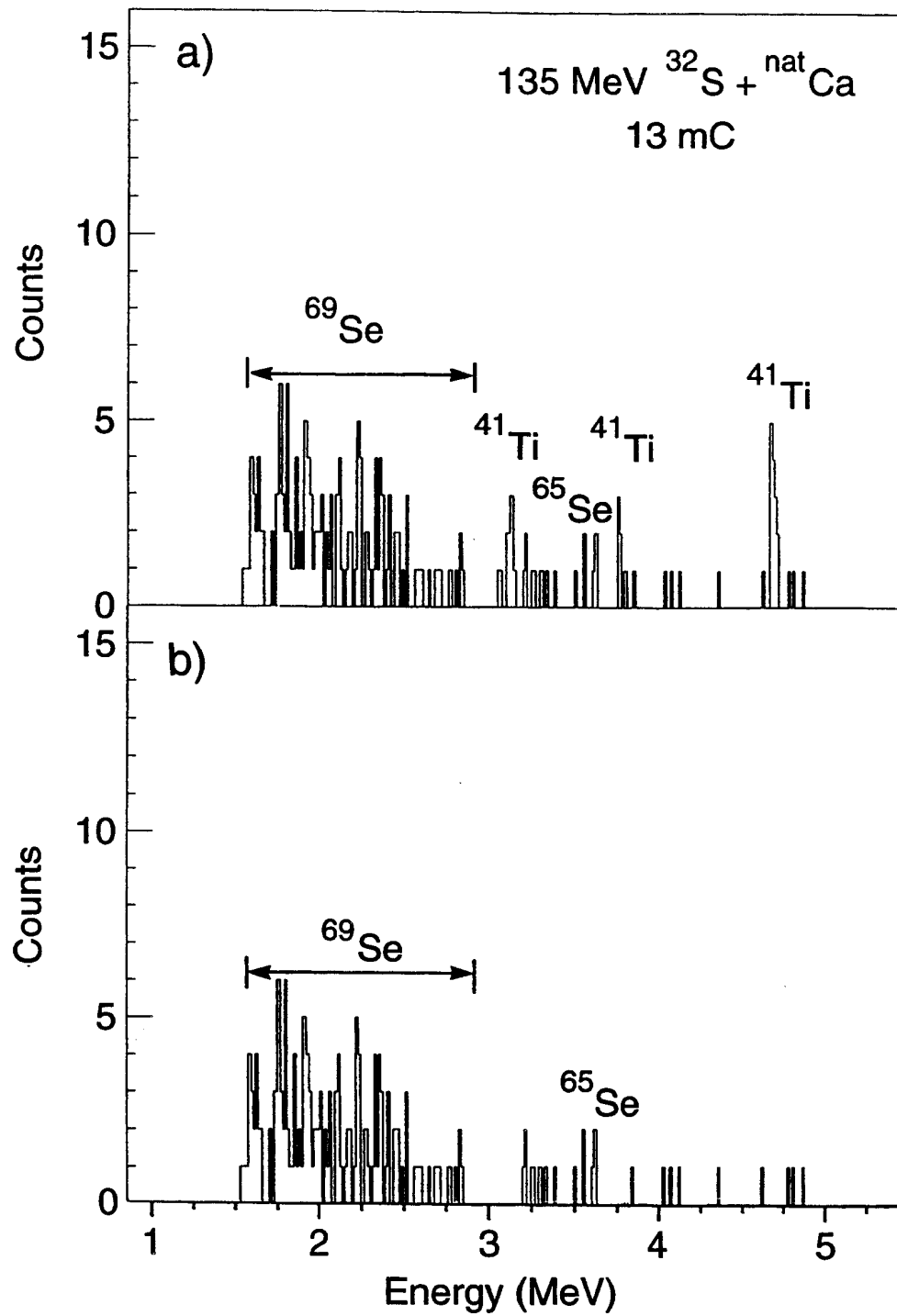
XBL 927-5748B



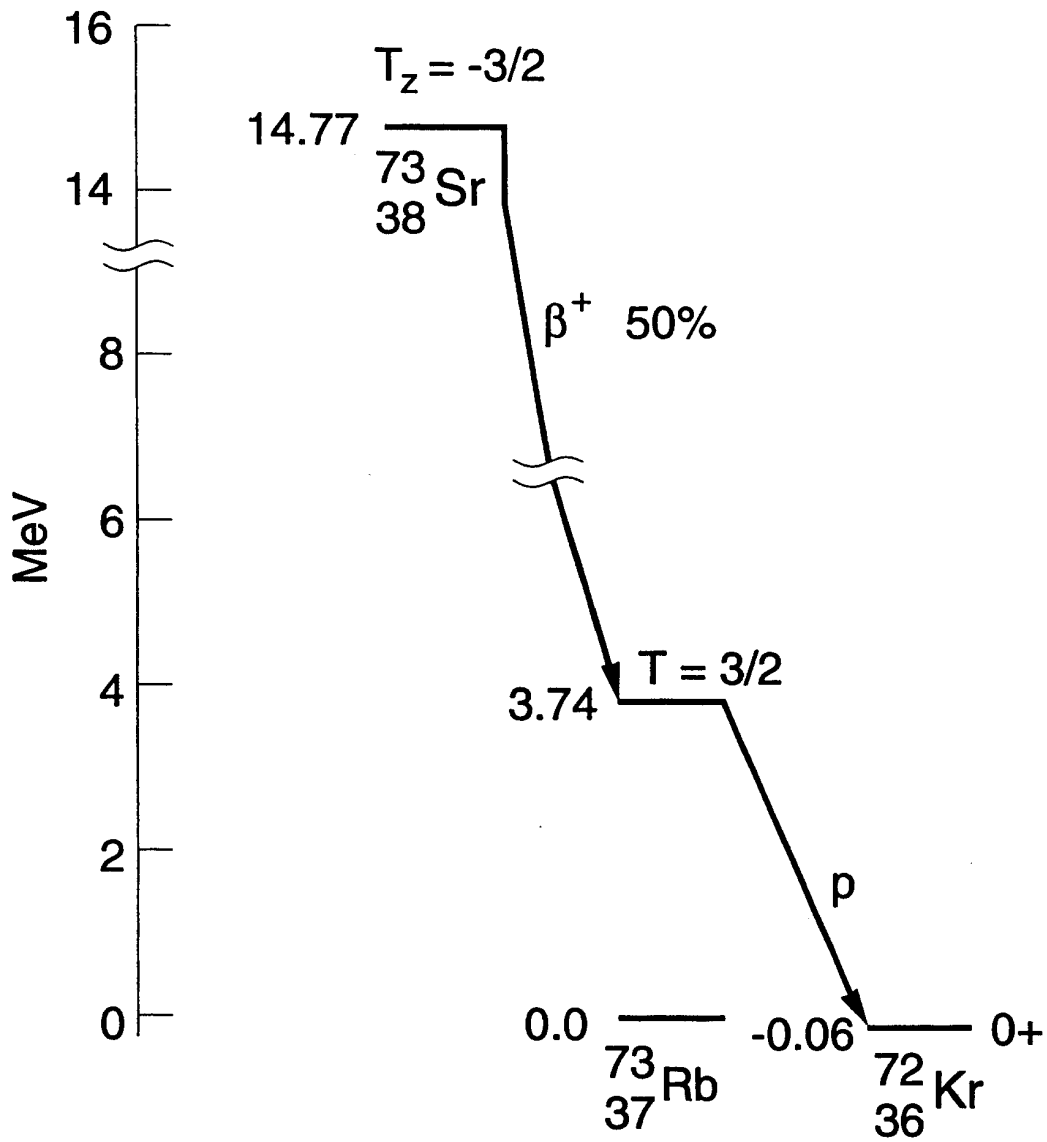
XBL 936-4055



XBL 936-4057



XBL 936-4056



$$E_p(\text{Lab}) = 3.75 \pm 0.05 \text{ MeV}$$

XBL 936-4053